Design and Simulation of High-throughput Microfluidic Droplet Dispenser for Lab-on-a-Chip Applications

Chenghui Jin[*1], Xingguo Xiong[2], Prabir Patra[1], Rui Zhu[1], Junling Hu[3]
[1]Department of Biomedical Engineering, [2]Department of Electrical and Computer Engineering,
[3]Department of Mechanical Engineering,
University of Bridgeport, Bridgeport, CT, USA
*Corresponding author: 170 Lafayette Street, Bridgeport, CT 06604, Email: chjin@my.bridgeport.edu

Abstract: Digital Microfluidic Biochips (DMFBs) have been widely used in Lab-on-a-Chip (LoC) for disease diagnosis and treatment applications. Biological sample to be processed are originally analog continuous flow. To convert it into digital droplets for DMFB processing, a microfluidic droplet dispenser acting as an analog-to-digital converter (ADC) is needed. In this paper, a high-throughput analog-to-digital microfluidic droplet dispenser is proposed. The proposed droplet dispenser has multiple digital output ports for parallel dispensing. COMSOL simulation is used to verify the function of the droplet dispenser. Multiphase flow model, laminar two-phase flow (tpf) and level set method are used in COMSOL simulation. The droplet dispenser can be used as interface between analog and digital microfluidic biochips.

Keywords: Digital microfluidic biochip (DMFB), microfluidic flow, analog-to-digital converter (ADC), droplet dispenser, Lab-on-a-Chip (LoC).

1. Introduction

Microfluidic biochips have attracted intense interest among researchers due to its low sample volume, low cost, low power consumption, fast response time and high efficiency [1]. Microfluidics has found applications in inkjet printer, DNA chips, lab-on-a-chip, micro drug delivery system, etc. [2] [3] [4]. According to the format of the microfluid being handled, microfluid biochips can be divided into two categories: analog microfluidic biochips (AMFBs) handle continuous flow (e.g. micropumps, microvalves, microchannels), while digital microfluidic biochips (DMFBs) manipulate discrete droplets. Most DMFBs utilize electrowetting-on-dielectric (EWOD) techniques to drive microfluidic droplets to move, split, merge, or perform other functions [5]. Microfluidic samples to be processed are generally continuous flow. Direct connection between continuous flow and EWOD network leads to two drawbacks: there is no droplet-volume control, and liquid excess cannot be evacuated in case of overpressure. In order for analog microfluid to be processed by DMFBs, an analog-to-digital converter (ADC) which can convert continuous flow into discrete digital droplets is required. Such ADC is actually a microfluidic dispenser which can dispense digital droplets from reservoir or continuous flow. Such droplet dispenser is essential for the integration of analog and digital microfluidic biochips into mixed-signal microfluidic biochips.

Research work about the microfluidic interface devices (analog-to-digital and digital-to-analog converters) are very few. In [6], a piezoelectrically actuated microfluidic droplet-dispensing chip was reported. It utilizes piezoelectric actuation to dispense droplets with volumes in the range of 50pL~1nL at ejection frequency of up to 6kHz. But the dispensed droplets are not directly connected to DMFB yet. In [7], an analog-to-digital microfluidic converter (ADMC) with passive valves for the conversion of a continuous liquid flow into digital droplets for EWOD actuation was reported. Valves calibration, geometry characteristics and losses reduction were optimized using COMSOL Multiphysics simulation. In [8], integration of digital microfluidics by EWOD and analog microfluidics by LDEP (liquid dielectrophoresis) in a single chip is reported. Three components for integrated digital and analog microfluidics were developed, which include a digital-to-analog converter, an analog-to-digital converter and a valve. In this research, the design and COMSOL simulation of a high-throughput microfluidic droplet dispenser (i.e. microfluidic analog-to-digital converter) is proposed. It has multiple digital output ports allowing alternating or parallel droplet dispensing. It can be used to convert analog continuous microfluidic flow into digital separate droplets for DMFB processing.

COMSOL simulation is used to verify the function of the droplet dispenser. Multiphase Flow Model, Laminar Two-Phase Flow (tpf) model and Level Set method are used in COMSOL simulation. The proposed microfluidic dispenser can be used for the system integration of analog and digital microfluidic biochips.

2. Microfluidic Dispenser Design

A microfluidic biochiop incorporating an analog-to-digital converter (droplet dispenser) used as interface between analog and digital microfluidic biochips is shown in Figure 1. Analog microfluidic flow coming out from micropump and micromixer is fed to the microfluidic analog-to-digital converter (ADC). The ADC takes the analog continuous flow as input, and converts it into digital microfluidic droplets. The droplets coming out from digital output ports are then fed to DMFB for further processing.

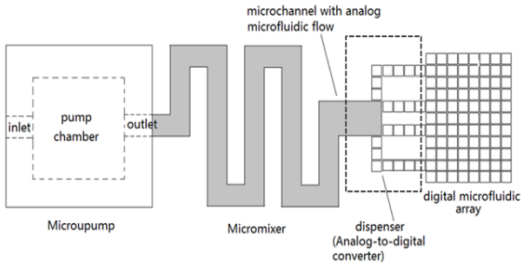

Figure 1. Microfluidic droplet dispenser connecting analog to digital microfluidic biochips

The structure design of the microfluidic droplet dispenser is shown in Figure 2. The analog microfluidic flow comes from pipette injection or the output of analog microfluidic devices (e.g. micropump, micromixer, microchannel, etc.). The droplet dispenser utilizes electrowetting to convert the continuous analog microfluidic flow into individual droplets. The size of the droplets is defined by the electrode size in the output ports. The droplet dispenser has multiple digital output ports. The output ports marked with number "1" and "2" can be activated in alternate or parallel mode. This allows multiple droplets to be dispensed at the same time for improved throughput.

3. Theoretical Analysis and Modeling

The movement of microfluidic droplets in DMFBs is based on electrwetting. In electrowetting, the wettability of an electrolytic

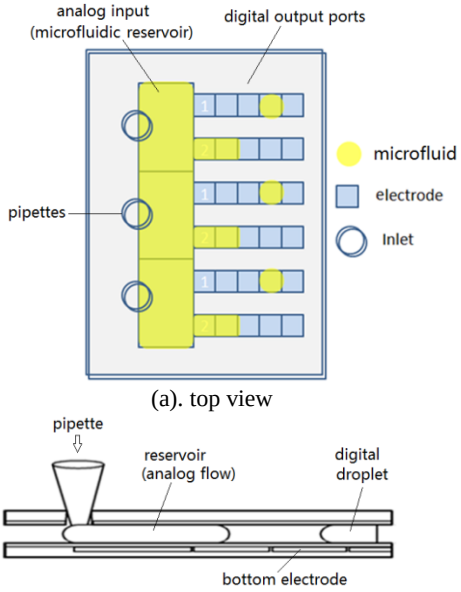

Figure 2. Design of microfluidic droplet dispenser. (a) Top view. (b) Cross-sectional view.

droplet on the surface of a hydrophobic dielectric layer can be modified by an external voltage applied between the droplet and the electrodes under the dielectric. When no voltage is applied, the relationship between contact angle θ_0 and the interfacial tensions of droplets on the solid surface is given by Young's equation [9]

$$\cos\theta_0 = \frac{\gamma_{sg}-\gamma_{sl}}{\gamma_{lg}} \qquad (1)$$

where γ_{sg} is the solid-gas interfacial tension, γ_{sl} the solid-liquid interfacial tension and γ_{lg} the liquid-gas interfacial tension. If a voltage V is applied between the droplet and the bottom electrode, the contact angles of the droplet will be changed to θ_V due to electrowetting. The relationship between the contact angle change and the applied voltage V can be described by Younng-Lippmann's equation [9]

$$\cos\theta_V = \cos\theta_0 + \frac{\varepsilon_r\varepsilon_0 V^2}{2t\gamma_{lg}} \qquad (2)$$

where ε_0 is the permittivity of vacuum, ε_r is the relative dielectric constant of the dielectric layer, and t is the thickness of the dielectric layer. Electrowetting can be used to drive microfluidic droplet in DMFB.

Droplet dispensing can be achieved by a combination of droplet moving and droplet splitting operations. Theoretical analysis and COMSOL simulation about droplet moving and

splitting can help us to understand the droplet dispensing, i.e. analog-to-digital conversion of microfluid.

3.1 Droplet Moving

The model of a droplet during transport with EWOD actuation is illustrated in Figure 3. A microfluidic droplet is sealed between top and bottom glass plates. The surfaces of both glass plates are hydrophobic to ease the movement of the droplet. There are embedded electrodes on both top and bottom glass plates. The top common electrode is grounded. The bottom electrodes are individually addressable and can be applied with driving voltage separately. The droplet is generally slightly larger than the bottom electrode, so it has small area overlap with next electrode. When a voltage V_d=V is applied to the next electrode, it causes imbalance in forces and drives the droplet to move toward it.

During transport the droplet maintains a dynamic contact angle θ_d. The force balance of the droplet decides the movement of the droplet. The net force f_A per unit length in site A along electrode surface toward right can be expressed as [10]

$$f_A = \gamma_{sg} - \gamma_{lg}\cos\theta_d - \gamma_{sl}(V) \qquad (3)$$

The net force f_B per unit length in site B along electrode surface toward right can be expressed as [10]

$$f_B = -\gamma_{sg} + \gamma_{lg}\cos\theta_d + \gamma_{sl}(0) \qquad (4)$$

The total driving force on the droplet per unit length along electrode surface is the sum of these two forces [10]

$$\begin{aligned} f_m &= f_A + f_B = \gamma_{sl}(0) - \gamma_{sl}(V) \\ &= \gamma_{lg}\,(\cos\theta_V - \cos\theta_0) \end{aligned} \qquad (5)$$

Under this net driving force, the microfluidic droplet will be driven to move toward the electrode in its right side. This is the working mechanism of droplet actuation in DMFB.

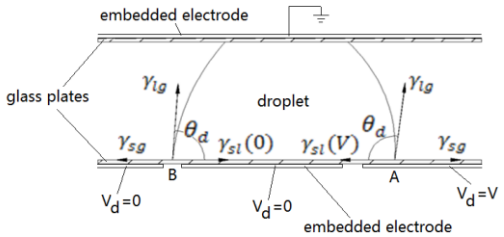

Figure 3. The force balance of a microfluidic droplet under EWOD actuation [9]

3.2 Droplet Splitting

In order to split a droplet into two, at least three electrodes are required. Figure 4 shows how a droplet can be split through EWOD. Initially the central electrode is activated, so the droplet is latched above central electrode. After that, the central electrode is deactivated, and both left and right electrodes are activated. Due to electrowetting, both left and right ends of the droplet have high wettability, while the middle portion of the droplet remains low wettability. This causes the droplet to be elongated along both sides of electrodes, but shrinks in the middle. As this trend continues, the droplet will eventually be split from the middle into two separate smaller droplets. According to the analysis in [10], the radii of curvature of microfluid droplet are linked to the contact angle difference by

$$\frac{R_2}{R_1} = 1 - \frac{R_2}{d}(\cos\theta_{b2} - \cos\theta_{b1}) \qquad (6)$$

where d is the channel gap, θ_{b1} is the contact angle on the bottom plate in the middle region of the droplet, θ_{b2} is the contact angle on the bottom plate in the end regions of the droplet. R1 and R2 are the principle radius of curvature in the middle region and end regions of the droplet respectively. Since θ_{b2} is the contact angle with driving voltage V applied, θ_{b1} is the contact angle without driving voltage (V=0), they are related to each other by Younng-Lippmann's equation

$$\cos\theta_{b2} = \cos\theta_{b1} + \frac{\varepsilon_r\varepsilon_0 V^2}{2t\gamma_{lg}} \qquad (7)$$

Substituting this into Equation (6), we have

$$\frac{R_2}{R_1} = 1 - \frac{R_2}{d}\left(\frac{\varepsilon_r\varepsilon_0 V^2}{2t\gamma_{lg}}\right) \qquad (8)$$

To form a necking in the middle of the droplet for successful droplet splitting, radius R_1 should be negative. In order to achieved this, we need to set $\frac{R_2}{d}\left(\frac{\varepsilon_r\varepsilon_0 V^2}{2t\gamma_{lg}}\right)$ to be large. That is, we can apply a large driving voltage V, or reduce the channel gap d, or set a large radius R_2 at both sides of the droplet (which means a larger control electrode size) [10]. In COMSOL simulation, we mainly control θ_{b2} (which is contact angle θ_V when voltage V is applied), θ_{b1} (which is contact angle

θ_0 when no voltage is applied), and γ_{lg} in order to accomplish droplet splitting.

In above analysis, contact angle saturation effect [11] is not considered. It is observed that there is an upper limit in the contact angle change due to EWOD. Once going beyond this limit, higher voltage does not further decrease the contact angle. The upper limit of contact angle change is observed to be around 60°~80° [11]. In COMSOL simulation, we need to ensure the contact angle change for droplet splitting is below this contact angle saturation limit.

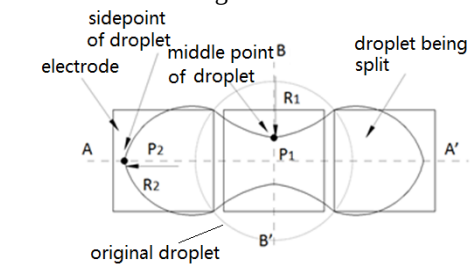

(a). top view

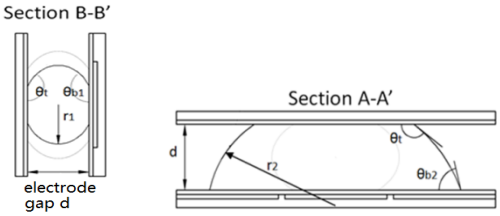

(b). (B-B') section view (c). (A-A') cross-setion view

Figure 4. Mechanism of droplet splitting [10]

4. COMSOL Simulation Results and Discussion

We used level set method in COMSOL simulation to study the interfacial motion of the multiphase flow. Microfluid is generally laminar flow with small Reynolds number. As a result, Laminar Two-Phase Flow, Level Set module were selected to perform this simulation. The Laminar Two-Phase Flow and Level Set method automatically set up the equations for the convection of the interface. The fluid interface is represented by the 0.5 contour of the level set function ϕ. In air $\phi = 0$ and in water $\phi = 1$. The level set function can thus be thought of as the volume fraction of water.

In COMSOL simulation, we developed 3D model of the microfluidic droplet dispenser. Some key parameters for the COMSOL simulation are listed as below. The contact angles were set as $\theta_0 = 120^\circ$ (contact angle without actuation voltage), and θ_V=60° (contact angle after actuation voltage is applied). The contact angle change is below the contact angle saturation limit. The size of electrode was 1mm×1mm, and three electrodes were used to split droplets. When a droplet can just be split, R2=-R1=0.5mm, $\cos\theta_{b2} = 60°$, and $\cos\theta_{b1} = 120°$. From equation (6) we can calculate the maximum channel gap d=0.25mm. For successful droplet splitting, we should set the gap d<0.25mm. In COMSOL simulation, we set d= 0.1mm, so that it allows lower driving voltage to be used for droplet splitting. The material properties and design parameters used in the COMSOL simulation are shown in Table 1 and 2.

Table 1. Fluid properties used in COMSOL simulation

Material Property	Oil (DP)	Water (CP)
Density (Kg/m^3)	1000	1000
Dynamic viscosity (mPa· s)	8	1.5

Table 2. Design parameters of droplet dispenser

Design Parameter	Value
Electrode size	1mm×1mm
Channel gap d	0.1mm
Liquid-gas interfacial tension γ_{lg}	0.05N/m
Relative dielectric constant ε_r of the dielectric layer	3.27
Dielectric layer thickness *t*	140nm
Actuation voltage V_d	22V
Inlet flow rate	0m/s
Outlet pressure	1×10^5Pa

4.1 COMSOL simulation: droplet moving and splitting

In order to prepare for the COMSOL simulation of microfluidic droplet dispenser, we first start with the COMSOL simulation of basic microfluidic manipulation: droplet moving and splitting. This helps us better understand the microfluidic behavior, and extract the important paramter - time settings for the COMSOL simulation. The proper timing for the actuation voltage sequence is vital to the success of droplet manipulation in COMSL simulation. Due to the complex behavior of microfluid, the simulation is time-consuming. It takes days to complete the simulation of the droplet manipulation. The COMSOL simulation result of droplet moving is shown in Figure 5. The actual droplet is marked as red color. The simulation shows detailed process for the droplet to move from original electrode to the next electrode in its right side. The droplet is first elongated due to electrowetting, and then completely dragged to

the next electrode. The whole process takes about 0.02sec to complete.

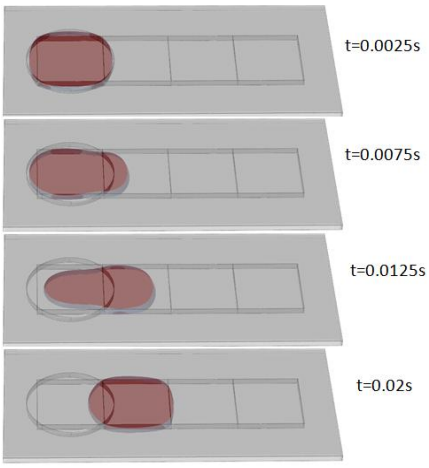

Figure 5. COMSOL simulation of droplet moving

COMSOL simulation of droplet splitting is shown in Figure 6. With the applied voltage sequence, the droplet is first elongated to both sides, forming a neck in the middle. The neck then begins to shrink, till finally it is broken in the middle. The whole process takes about 0.0225sec to complete.

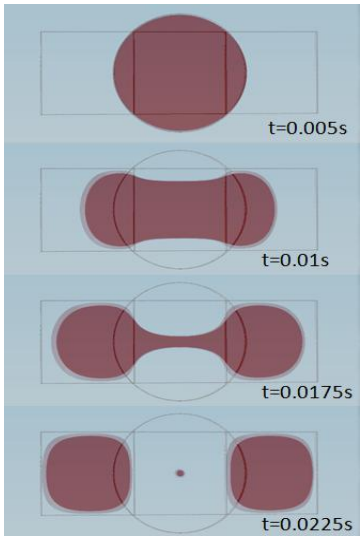

Figure 6. COMSOL simulation of droplet splitting

From simulation result in Figure 6 we see that the droplet was not split perfectly - a small residue (shown as small red dot) was left in the middle after splitting. This residue is undesirable and it may cause contamination to the following droplet manipulation. In [12], it was supposed that the large EWOD force causes the droplet to be pulled apart so fast, so that the middle region was never able to become a thin neck. This may in turn form the residue in between. In our 3D COMSOL simulation, we find that even the middle region does form the thin neck, it still causes residue in the middle. We looked into the detailed process of the residue formation in COMSOL simulation. The localized zoom view in Figure 7 shows the formation of the residue. We can see that as the neck in the middle becomes thinner, a double convex meniscus is formed in the middle region of the droplet above the central non-activated electrode. Once the neck region continues to shrink, this double convex meniscus eventually forms the small residue after splitting. If the channel gap is much lower than necessity or if θ_V is much smaller than necessity, the middle region forms the double convex meniscus more easily. The residue can be eliminated by utilizing contact angle saturation effect [12]. We verified this in COMSOL simulation by increasing the channel gap (d) from 0.1mm to 0.25mm, and did observe that the residue disappeared. After trying many different settings, we finally found an effective way to eliminate the residue in droplet splitting. We set the actuation voltage sequence as:

[left, middle, right]=[on, on, off] →[on, off, on]

Instead of dragging the droplet from both ends simultaneously, this voltage scheme holds the droplet in left side, and then drags the droplet from left to right gently to split it. This is similar to the process of droplet dispensing. By doing so, we can effectively eliminate the residue in droplet splitting, but the volume of two small droplet after splitting may not be exactly equal.

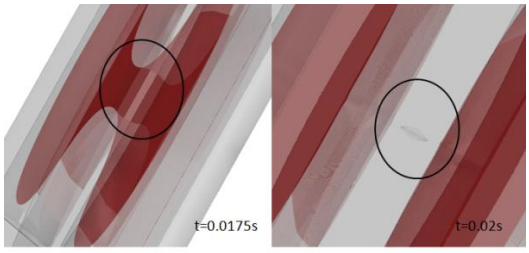

Figure 7. Cross-section view of droplet splitting showing the residue after splitting

4.2 COMSOL simulation of microfluidic analog-to-digital dispenser

To reduce the simulation time, we simulate a microfluidic droplet dispenser with only two digital output ports. During COMSOL simulation of droplet moving/splitting, we found the total volume of droplet is reduced when

using Level Set module to study the interfacial motion of the oil and water. This volume loss problem become even more significant for droplet not in motion. It was pointed out in [12] that the level set would become distorted and introduce numerical inaccuracies, which might be the reason for the droplet volume loss. We tried COMSO Phase Field module as well, and it won't help the problem. Finally, we solved this problem by using finer mesh (from Fluid Dynamics Normal to Fluid Dynamics Finer). This results in much longer simulation time (about five times longer) in COMSOL simulation, but the droplet volume loss is avoided. In COMSOL simulation of droplet dispenser, we only used finer mesh for the last two electrodes for each output ports to reduce the number of nodes for faster simulation. The meshed model of droplet dispenser in COMSOL is shown in Figure 8. For the initial conditions to settle, we wait 0.005sec before the electrodes were activated.

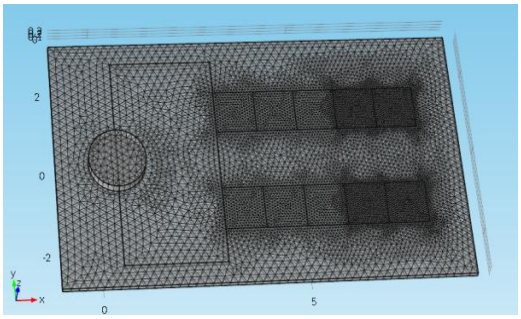

Figure 8. Geometry of droplet splitting

We first activate the droplet dispenser in alternate working mode. The COMSOL simulation result is shown in Figure 9. As seen in Figure 9, microfluid elongates to the 3rd electrode of the top output port at time t=0.035sec and dispense a complete droplet at t=0.04sec. The dispensed droplet is then moved to the right end of output port and kept there for the rest of the time in simulation since we did not set an outlet for water droplets. The electrodes of the bottom output port are then actuated, and the second droplet is completely dispensed at time t=0.065sec. We found the volume of the first droplet is smaller than the second one. However, if we continue the dispensing, the size of following droplets will be the same as the second droplet. Only the first droplet is smaller. This indicates that it takes some time for the droplet dispensing to become stable. The overall dispense rate is about one droplets per 0.025sec(0.065s-0.04s).

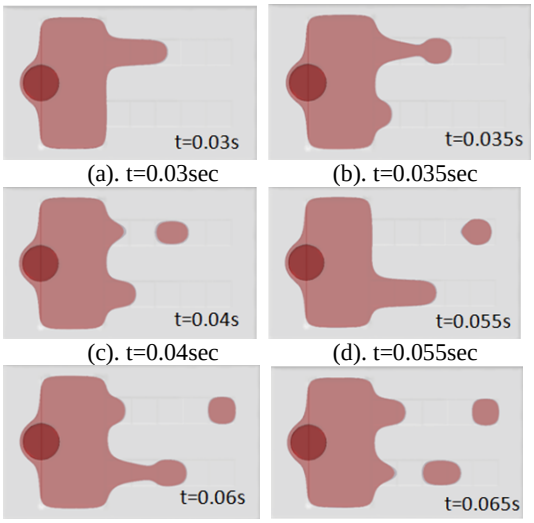

(a). t=0.03sec (b). t=0.035sec
(c). t=0.04sec (d). t=0.055sec
(e). t=0.06sec (f). t=0.065sec

Figure 9. COMSOL simulation of droplet dispenser in alternate mode

Figure 10 shows the microfluidic flow rate in inlet, top and bottom output ports. From the figure, we can see droplets are dispensed from analog reservoir to top and bottom output ports alternately. Furthermore, the peak of the first droplet from top output port is smaller than the peak from bottom output port, but the second peak of top port becomes equal to that of the bottom port. This is in good agreement with what we observed in Figure 9. The first droplet is smaller and then the dispensing become stable.

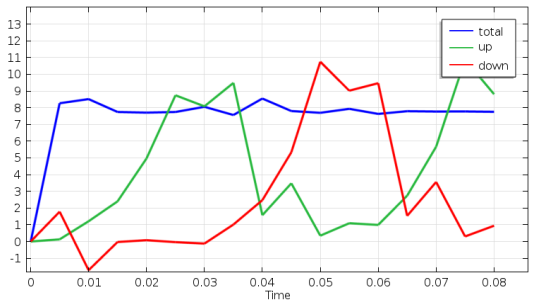

Figure 10. Flow rate of inlet ("total"), top port ("up") and bottom port ("down").

We also simulated the droplet dispenser in parallel working mode. The result is shown in Figure 11. As seen in the figure, microfluid is elongated to the third electrode in output ports at t=0.04sec, and the first droplets from both top and bottom output ports are completely dispensed at t=0.06sec. However, the next droplets cannot be dispensed immediately, they should wait the previous droplets move from the 3rd electrodes. As a sequence, the dispense rate is slower than two droplets per 0.06sec(here, we

set the repeat time as 0.07s). Furthermore, both droplets have the same volume. That is, it does not suffer the droplet size reduction for the first droplet as in the alternate working mode.

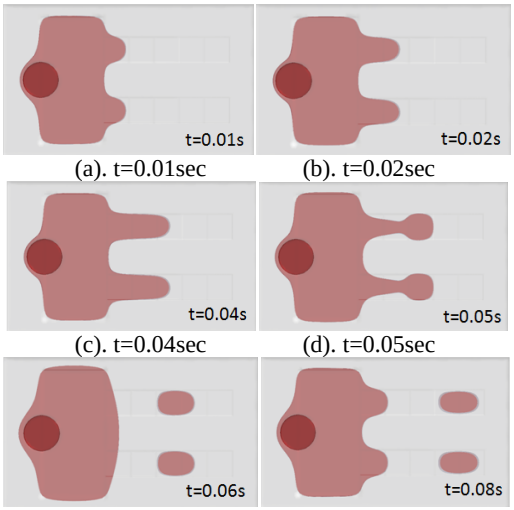

(a). t=0.01sec (b). t=0.02sec

(c). t=0.04sec (d). t=0.05sec

(e). t=0.06sec (f). t=0.08sec

Figure 11. COMSOL simulation of droplet dispenser in parallel mode

5. Conclusions

In this paper, the design and simulation of a microfluidic analog-to-digital droplet dispenser for Lab-on-a-Chip application is proposed. The proposed droplet dispenser has multiple digital output ports. Taking analog microfluid flow as input, the dispenser can convert it into separate digital droplets for DMFB processing. COMSOL simulation is used to understand the mechanism of dispensing and verify the function of the device. The droplet dispenser can work in both alternate and parallel modes. It can be used for integration of analog and digital microfluidic biochip into a single Lab-on-a-Chip.

6. References

[1] F. Su, K. Chakrabarty and R. Fair, "Microfluidics-Based Biochips: Technology Issues, Implementation Platforms, and Design-Automation Challenges," *Computer-Aided Design of Integrated Circuits and Systems, IEEE Transactions on*, vol. 25, no. 2, pp. 211-223, 2006.

[2] D. N. Breslauer, P. J. Lee and L. P. Lee, "Microfluidics-based systems biology - Molecular BioSystems," *Molecular Biosystems*, vol. 2, pp. 97-112, 2006.

[3] V. Srinivasan, V. K. Pamula, M. G. Pollack and R. B. Fair, "Clinical diagnostics on human whole blood, plasma, serum, urine, saliva, sweat, and tears on a digital microfluidic plattform," in *Proc. of MicroTAS*, 2003.

[4] H. Moon, A. R. Wheeler, R. L. Garrell, J. A. Loo and C.-J. Kim, "An integrated digital microfluidic chip for multiplexed proteomic sample preparation and analysis by MADDA-MS," in *Lab on a Chip*, 2006.

[5] M. Pollack, A. Shendorov and R. Fair, "Electrowetting-based actuation of droplets for integrated microfluidics," *Lab on a Chip*, vol. 2, pp. 96-101, 2002.

[6] M. J. Ahamed, S. Gubarenko, R. Ben-Mrad and P. Sullivan, "A Piezoactuated Droplet-Dispensing Microfluidic Chip," *Microelectromechanical Systems, Journal of*, vol. 19, no. 1, pp. 110-119, 2010.

[7] R. Dufour, C. Wu, F. Bendriaa, V. Thomy and V. Senez, "Analog to digital microfluidic converter," in *Proceedings of the COMSOL Conference*, Milan, 2009.

[8] Y.-C. Lin, K.-C. Chuang, T.-T. Wang, C.-P. Chiu and S.-K. Fan, "Integrated Digital and Analog Microfluidics by EWOD and LDEP," in *Nano/Micro Engineered and Molecular Systems, 2006. NEMS '06. 1st IEEE International Conference on*, Zhuhai, China, 2006.

[9] F. Mugele and J. Baret, "Electrowetting: from basics to applications," *Journal of Physics: Condensed Matter*, vol. 17, pp. R705-R774, 2005.

[10] S. K. Cho, H. Moon and C. J. Kim, "Creating, Transporting, Cutting and Merging Liquid Droplets by Electrowetting-Based Actuation for Digital Microfluidic Circuits," *Journal of MicroElectroMechanical System*, vol. 12, pp. 70-80, 2003.

[11] V. Peykov, A. Quinn and J. Ralston, "Electrowetting: a model for contact-angle saturation," *Colloid Polymer Sci.*, vol. 278, p. 789–793, 2000.

[12] S. W. Walker and B. Shapiro, "Modeling the Fluid Dynamics of Electrowetting on Dielectric (EWOD)," *Journal of Microelectromechanical Systems*, vol. 15, pp. 986-1000, 2006.